Mon. Not. R. Astron. Soc. **357,** 819–833 (2005) doi:10.1111/j.1365-2966.2005.08608.x

The dwarf low surface brightness galaxy population of the Virgo Cluster – II. Colours and H I line observations

S. Sabatini,[1,2]★ J. Davies,[1] W. van Driel,[3] M. Baes,[1,4]† S. Roberts,[1] R. Smith,[1] S. Linder[1] and K. O'Neil[5]

[1]*Department of Physics and Astronomy, Cardiff University, Queen's Building, PO Box 913, Cardiff CF24 3YB*
[2]*INAF-OAR, via di Frascati 33, 00040 Monteporzio Catone, Roma, Italy*
[3]*Observatoire de Paris, GEPI, CNRS UMR 8111 and Université Paris 7, 5 place Jules Janssen, F-92195 Meudon Cedex, France*
[4]*Sterrenkundig Observatorium, Gent, Belgium*
[5]*NRAO, PO Box 2, Green Bank, WV 24944, USA*

Accepted 2004 November 5. Received 2004 September 10; in original form 2004 February 19

ABSTRACT

In order to investigate the nature of dwarf low surface brightness (LSB) galaxies we have undertaken a deep *B*- and *I*-band CCD survey of a 14-deg^2 strip in the Virgo Cluster and applied a Fourier convolution technique to explore its dwarf galaxy population down to a central surface brightness of $\sim$26 *B* mag arcsec^{-2} and a total absolute *B* mag of ~ -10. In this paper we carry out an analysis of their morphology, $(B - I)$ colours and atomic hydrogen content. We compare these properties with those of dwarf galaxies in other environments to try and assess how the cluster environment has influenced their evolution. Field dwarfs are generally of a more irregular morphology, are bluer and contain relatively more gas. We assess the importance that various physical processes have on the evolution of cluster dwarf galaxies (ram-pressure stripping, tidal interactions, supernova-driven gas loss). We suggest that enhanced star formation triggered by tidal interactions is the major reason for the very different general properties of cluster dwarfs: they have undergone accelerated evolution.

Key words: galaxies: clusters: individual: Virgo Cluster – galaxies: dwarf.

1 INTRODUCTION

The effect of the environment upon bright galaxies has been well studied over the years but can still be controversial (see for example the E-to-S0 ratio controversy: Dressler et al. 1997; Andreon 1998; Lubin et al. 1998). There are noticeable variations in the morphology, colour and magnitude of cluster bright galaxies with respect to the properties of field galaxies. A galaxy in a cluster can be subject to many different processes that are not at work (or less likely to occur) in the field: direct collisions, galaxy–galaxy or galaxy–cluster tidal interactions, high/low-speed encounters between galaxies, ram-pressure stripping by the intracluster medium (ICM), pressure confinement and combinations of the above. The two main effects produced by these various processes are in some ways opposite: if, on the one hand, a cluster can diminish the gas content (and thus the star formation rate, SFR) of its galaxies by means of various stripping mechanisms, on the other hand it can also trigger star formation and accelerate evolution by means of tidal interactions. Which of these two effects is prominent remains controversial (Davies & Phillipps 1989; Hashimoto et al. 1998; Gnedin 2003) and possibly depends on the exact nature of the environment and on the galaxy type considered. Different studies come to different conclusions: whereas some report the quenching of star formation in clusters rather than its enhancement (Kennicutt 1983; Dressler, Thompson & Shectman 1985; Poggianti et al. 1999; Dressler et al. 1999), others find the opposite result, suggesting a similar or higher SFR in clusters than in the field (see Bothun & Dressler 1986; Caldwell et al. 1993, for the Coma Cluster).

In addition, observations of the distant 'faint blue galaxies' have been used to infer that star formation is enhanced (or accelerated) as galaxies initially fall into a cluster, but at the current time star formation is suppressed compared to the field.

These issues are further complicated when investigating the effects of the environment upon dwarf galaxies, owing to their low magnitude and surface brightness values. If dwarfs are the first objects formed, as predicted by cold dark matter (CDM) models of hierarchical structure formation (White & Rees 1978; White & Frenk 1991), we should expect them to be the oldest galaxies in the Universe and to be present in all environments. They should have

★E-mail: sabatini@mporzio.astro.it
†Postdoctoral Fellow of the Fund for Scientific Research, Flanders, Belgium (FWO-Vlaanderen).

similar properties everywhere, unless the environmentally dependent evolution is strong. The latest observational results, however, indicate that the faint-end-slope of the luminosity function (LF; which quantifies the number of dwarfs) has a strong environmental dependence (Trentham & Tully 2002; Roberts et al. 2004). If the stellar mass of a dark halo is proportional to its dark matter mass, then the LF is a direct measure of the dark matter mass function and model predictions require many more small dark matter haloes around individual galaxies and in galaxy clusters than have been detected (Kauffmann, White & Guiderdoni 1993; Moore, Lake & Katz 1998). This failure of the standard CDM prediction is not universal: there are galaxy clusters, like Coma, Virgo and Fornax, where the faint-end slope of the LF is found to be steep (Kambas et al. 2000; Milne & Pritchet 2002; Sabatini et al. 2003). Compared to these clusters, there is a real lack of low-luminosity galaxies in lower density environments, like the Local Group and the field (Pritchet & van der Bergh 1999; Norberg et al. 2002; Roberts et al. 2004). These results imply that there cannot be a global dwarf galaxy formation suppression mechanism as is invoked in many simulations. This normally takes the form of gas loss through supernova (SN) driven winds (a 'feedback' mechanism).

Ignoring the possibility of many dark haloes with no baryons at all, there are two possible interpretations consistent with the observations as follows.

(1) CDM predictions are correct, but we need to invoke some mechanisms that preserve primordial dwarf galaxies in some environments, while destroying them in others.

(2) The dwarf galaxies found in rich clusters are a different population from the primordial one predicted by CDM – meaning that some processes must have actually formed them solely in some environments and/or suppressed them in others.

The most popular environment dependent mechanisms proposed in support of the former hypothesis are as follows.

(a) Squelching (Tully et al. 2002) – a suppression of dwarf galaxy formation in low-density environments owing to photoionization occurring at a critical phase in the structure formation. Note, however, that WMAP results now place the ionization epoch at $z \approx 20$ (Spergel et al. 2003) and fluctuations of order $10^7\,M_\odot$ in CDM models are extremely rare at that epoch (Miralda-Escude 2003). In addition, the star formation histories of Local Group satellites show evidence of several (also recent) star formation bursts, some continuing to the present day. For these reasons we will not consider this process further.

(b) Pressure confinement (Babul & Rees 1992) – the pressure of the ICM reduces the gas loss produced by a feedback mechanism such as SN-driven winds.

On the other hand, in support of the second hypothesis, mechanisms that can form dwarf galaxies after the CDM dwarf galaxy formation epoch are as follows.

(c) Tidal interactions (Okazaki & Taniguchi 2000) – galaxy–galaxy interactions and mergers can result in the formation of so-called tidal dwarfs.

(d) Harassment (Moore et al. 1999) – infalling LSB disc galaxies in a cluster are subject to many high-speed encounters that can result in their morphological transformation into dwarf Ellipticals (dE) galaxies.

Trying to disentangle these issues requires a better understanding of how the mechanisms involved in galaxy evolution relate to the environment, and thus a detailed study of the properties of the dwarfs found in different environments: in what follows we will try to analyse what makes a cluster different from the field or from a loose group, and which observables (e.g. galaxy colours, H I content, velocity dispersion) can help distinguish between the two different interpretations stated above.

Being the nearest cluster ($d \sim 16$ Mpc; Graham et al. 1999; Jerjen et al. 2004) with several hundreds of bright galaxies [$\sim$1277 sure members are listed in the Virgo Cluster Catalogue (VCC); Binggeli, Sandage & Tarenghi 1984], the Virgo Cluster offers the best opportunity for the detailed study of large numbers of bright galaxies and faint dwarfs in the cluster environment. The most complete optical survey of the Virgo Cluster to date, the VCC, compiled using photographic plates and a visual detection method, is complete for objects of moderate surface brightness with $M_B < -14$. At present, however, there is no published catalogue of candidate dwarf galaxy members of the entire Virgo Cluster which is complete for objects fainter than $M_B = -14$ and central surface brightness values as low as $26\,B$ mag arcsec^{-2}. These are the properties of the numerous low-luminosity galaxies dominating the numbers in the Local Group (Mateo 1998).

There are several studies in the literature that point to evolving populations of dwarfs in clusters of galaxies (see Conselice, Gallagher & Wyse 2001; Poggianti et al. 2001; Conselice et al. 2003a; Jerjen, Binggeli & Barazza 2004; Rakos & Schombert 2004), but none of them reaches the faint magnitude values of Local Group dwarfs. To investigate the possibility that previous surveys have missed a fainter population of Virgo Cluster dwarfs, we have applied (Sabatini et al. 2003; paper I) an optimized Fourier convolution technique to deep CCD images of one strip in the cluster, detecting LSB dwarfs in the B band down to surface brightness values of 26 mag arcsec^{-2} and absolute magnitudes of -10 at the assumed Virgo Cluster distance. A detailed description of the selection procedure and a determination of the LF of the cluster dwarfs is given in paper I. Over a search area of $\sim$14 deg^2 we have identified 231 dwarf low surface brightness (LSB) candidates, 105 of them being previously uncatalogued galaxies (see VCC; Impey, Bothun & Malin 1988; Trentham & Hodgkin 2002).

With all this in mind, and with the aim of improving our understanding of the nature of very faint dwarf galaxies in the cluster environment, we have supplemented our deep B-band data with I-band data and H I line follow up observations. In a separate paper (Roberts et al. 2004) we compare our results with those from an identical data set (same detector, telescope, exposure time, detection method) of both the Ursa Major Cluster and the general field.

The paper is organized as follows: in Sections 2 and 3 we describe the data and the data reduction; in Section 4 we discuss the spatial distribution of the dwarf galaxies and its relation with the giants; in 5 we present the $B - I$ colours of the galaxies in our sample and compare these results with different environments of the Local Universe; in Section 6 we describe the Arecibo 21-cm H I line observations, data reduction and results of the subsample observed; in Sections 7 we discuss the possible mechanisms occurring in the cluster environment and their relation with our results; in Section 8 we give our conclusions.

2 THE DATA

The optical data that we use in this paper are part of the 2.5-m Isaac Newton Telescope Wide Field Camera (INT WFC) survey of the Virgo Cluster (see paper I for further details). Here we present results

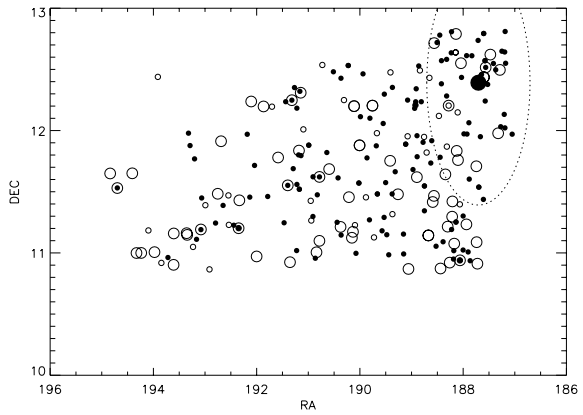

Figure 1. Detections in the strip. Different symbols refer to different morphologies: filled circles for dE, small open circles for dI and larger open circles for VLSB, a circle around a dot indicates an undecided dE/dI. The large filled dot near the top right corner is M87. We plotted a 1-deg radius circle around M87 to show the area where our H I observations were too highly contaminated by this 220-Jy continuum source. The RA and Dec. axes are in decimal degrees; the aspect ratio of the field is stretched in the north–south direction – see the plotted circle.

from the west–east *B*- and *i*-band strip in the cluster, extending from the centre of the cluster (identified as M87) eastwards for 7°, with a total area of $\sim$14 deg^2. This region of the cluster is part of the dynamical unit named cluster A (M87), excluding members of other units like cluster B, clouds M and W.

The data in both bands were preprocessed and fully reduced using the Wide-Field Survey pipeline: this includes de-biasing, bad pixel replacement, non-linearity correction, flat-fielding, defringing (for *i* band) and gain correction. The photometric calibration makes use of several (5–10 per night) standard stars and the zero points are accurate to 1–2 per cent. For more details, see http://www.ast.cam.ac.uk/wfcsurv/pipeline.html. The results throughout the paper are given in the *B* and *I* magnitudes of the Johnson–Cousin photometric system and the conversion from the INT colours was done using instructions given at http://www.ast.cam.ac.uk/wfcsurv/colours.php.

In paper I we presented a convolution technique to detect and also measure the photometric properties of faint LSB galaxies. By applying it to the *B*-band data, we obtained a final catalogue of 231 dwarf galaxy candidates in the strip (Fig. 1). The use of this automated technique on homogeneous deep data allows us to study the population of Virgo Cluster dwarf galaxies down to the very faint limiting central surface brightness values ($\sim$26 *B* mag arcsec^{-2}) and absolute magnitudes ($M_B \sim -10$) typical of Local Group galaxies.

3 DATA REDUCTION

For the analysis of $(B - I)$ colours, we need consistent measurements of the magnitudes in both bands. Even when fully reduced, the *i*-band images are still affected by a fringing signature. This makes it impossible to apply our convolution technique to measure fluxes in this band. The data analysis for this section was therefore performed using the aperture photometry routine from the GAIA package on both the *i* and *B*-band data for the sake of consistency. Photometry was done using for each galaxy an aperture large enough to include its total flux and yet avoiding contamination by nearby objects. For each object the aperture and centre position determined in the *B* band was subsequently also used in the *i* band.

Although morphological classification is very difficult for some of the objects, owing to their very low surface brightness, we classified the galaxies of our sample either as dE, dI or VLSB (very low surface brightness). We describe as dE the spherical diffuse galaxies and the more compact elliptical objects; dE,N denotes objects in this category that show a nucleus. The dIs are the irregularly shaped objects, often showing clumps. The objects that could not be assigned to either of these category we refer to as VLSB. The overall sample is dominated by dE types (54 per cent, a quarter of which have a nucleus), whereas the dIs represent 27 per cent and the VLSBs 14 per cent.

$B - I$ colours were measured for practically all the galaxies, with the exception of six; three have very low signal-to-noise ratios on the *B*-band images and are not visible at all on the *i*-band images; for the other three the *i*-band image is corrupted. For the errors on the $B - I$ colours we refer to Section 5 and for more detailed comments on single objects to Section 6.3.

The total *B* magnitudes and central surface brightness values used in the plots were all calculated using our convolution algorithm (see paper I for estimated errors).

4 THE DWARF-TO-GIANT RATIO

In paper I we have shown the radial profile of the galaxy number density of our sample. This can be compared with that of the bright galaxies. We have defined a dwarf-to-giant ratio (DGR) as the ratio of dwarf galaxies (defined as those with $-14 \leqslant M_B \leqslant -10$) to giant galaxies (with $M_B \leqslant -19$[1]). This is a simpler and more versatile measure for quantifying the luminosity distribution than the LF. We have shown that the DGR remains rather flat with distance from M87 with a median value of $\sim$20. This number has to be compared with a value of about 6 for the field population (Roberts et al. 2004).

It is difficult to compare our results with other studies, as different papers use different definitions for the DGR. Ferguson & Sandage (1991) studied seven groups and clusters and defined an elliptical giants-to-dwarf ratio (EDGR). Our results are consistent with the strong correlation found by these authors of the EDGR with the cluster richness: they also found that the EDGR in the Virgo Cluster appears to be independent of distance from the cluster centre. Secker & Harris (1996), however, find an EDGR in the Coma Cluster identical to the one in the less rich Virgo Cluster and thus in contrast with the EDGR-richness correlation. They point out that the presence of substructure could be an important factor and that the Coma Cluster result would be consistent with the cluster being built up from the mergers of less rich clusters. In addition, more recently, Driver et al. (1998) studied seven rich clusters at redshift $\sim$0.15 and found an anti-correlation between richness (or density) of the cluster and DRG; their definition of dwarfs, however, comprise all galaxies fainter than -19.5 and it is therefore difficult to compare their results with ours.

Our results have also to be compared to the values in the Local Group: in a hierarchical structure formation scenario, clusters like Virgo, should be formed by accretion of smaller groups. It is thus possible that some or all the dEs in Virgo were once part

[1] This definition for the giants is assumed in order to easily compare our numbers with the ones in the Local Group, as this is the magnitude limit to include its three giants M31, M33 and the Milky Way.

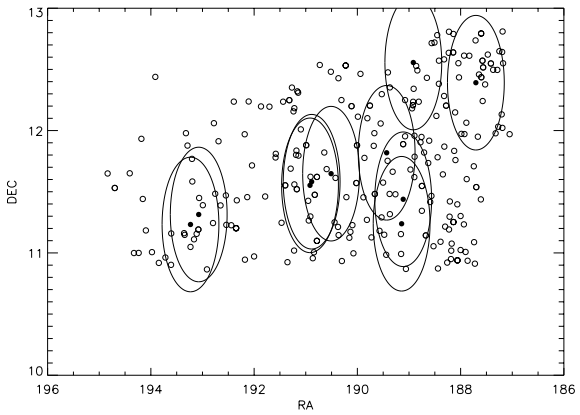

Figure 2. Spatial distribution of the dwarf galaxies of our sample (open circles) and of the giant galaxies of the Virgo Cluster (dots), defined as the ones with $M_B \leqslant -19$. Large circles are the tidal radii of the giant galaxy that is at their centre.

of structures like the Local Group that fell into Virgo with their spirals and satellites. The *expected* DGR from hierarchical structure formations, should be the same for all these environments, or a smaller one in the cluster if the disruptive processes are the dominant ones for dwarf galaxies, as often assumed in ΛCDM models of galaxy formation. Contrary to these predictions, the *observed* increase in the DGR that we find in clusters would instead imply that some galaxies are actually 'formed' in the assembling of the cluster.

Dwarfs in the Local Group are mainly associated with bright galaxies: 75 per cent of them cluster in three subgroups respectively around M31, the Milky Way and NGC 3109 and the other 25 per cent are part of the Local Group Cloud, populated only by dwarf irregular systems (Mateo 1998). It is interesting to compare these properties with the spatial distribution that we find in the Virgo Cluster. Fig. 2 shows the spatial distribution of our sample dwarfs and of the Virgo Cluster giants ($M_B \leqslant -19$) from the VCC. We have also plotted the tidal radius around each giant galaxy in the strip (larger circles). This is the truncation radius of the dark matter haloes in the cluster and it can therefore be considered as the one within which subhaloes remain bound to the galaxy potential well. Describing the cluster and the galaxy haloes with a singular isothermal distribution,[2] the tidal radius R_t can be approximated as:

$$R_t \approx \frac{\sigma_g}{\sigma_{cl}} R_p \qquad (1)$$

where R_p is the distance of the closest approach to the centre of the cluster, and σ_g and σ_{cl} are respectively the velocity dispersions of the galaxy and of the cluster (Merritt 1984; Gnedin 2003). For many galaxies the distance of the closest approach to the cluster centre is of order of the cluster core radius (Gnedin 2003) and for the Virgo Cluster we can therefore approximate it with 0.5 Mpc (Binggeli et al. 1987). Assuming the velocity dispersion of the galaxies in the cluster to be $\sim$700 km s^{-1} and the rotational velocity of a giant $\sim$200 km s^{-1}, the typical tidal radius for a giant galaxy in the Virgo Cluster is $R_t \sim 150$ kpc.

[2] Whether the Virgo Cluster is relaxed is still a matter of debate (see Binggeli, Tammann & Sandage 1987; Binggeli, Popescu & Tammann 1993; Schindler et al. 1999); nevertheless substructures in the cluster will amplify the truncation effect (Gnedin 2003) and would therefore reduce the radii of the circles in Fig. 2.

Although the spatial distribution in Fig. 2 is just a projection and it is difficult to know what the real distribution is, it is interesting that a significant part of the dwarf galaxy population does not seem to be associated with the giants. A similar result was found by Ferguson (1992): in his analysis of bound companions in the Virgo Cluster, he suggested the existence of a free-floating cluster member population made of stripped companions. In agreement with this view, a more recent paper by Conselice et al. (2001) showed that there is little evidence for a dynamically cool dE component, as might be expected if a significant fraction of dE were bound to individual cluster galaxies (see also Binggeli et al. 1987; Binggeli et al. 1993). Our results also indicate that there appears to be a cluster dwarf population: ∼40 per cent of the galaxies in our sample are apparently not bound to the giants and this is a larger number than that in the Local Group. Again this number cannot be accounted for if the Virgo Cluster was simply made up of groups like the Local Group. Also, after subtracting the average number density of this 'unbound' dwarf population from the average number of dwarf galaxies within a projected tidal radius from a giant, the number of dwarfs possibly associated with each giant is $\sim 13 \pm 3$. This has to be compared with a value of 3 for the Milky Way (this would be obtained if the Milky Way was at the Virgo Cluster distance and for dwarf galaxies that match our selection criteria) and 4 for the Local Group, suggesting that infalling galaxy groups cannot supply sufficient dwarfs in a cluster (see also Conselice et al. 2001; Tully et al. 2002).

5 $B-I$ COLOURS

Being interested in the nature of the dwarf galaxies in our sample and in possible environmental effects on the evolution of galaxies in the cluster, we first investigated the possibility of a relationship between colours and cluster-centric distance. In Fig. 3 we plot the $B-I$ integrated colours of our galaxies as a function of their position in the cluster (identified as the distance from M87); different symbols refer to different morphologies: filled dots for dEs and open diamonds for dIs and VLSBs. The range of colours is quite wide, with an average value of about 1.7. Even if this figure shows that the colours do not appear to have any dependence upon distance from

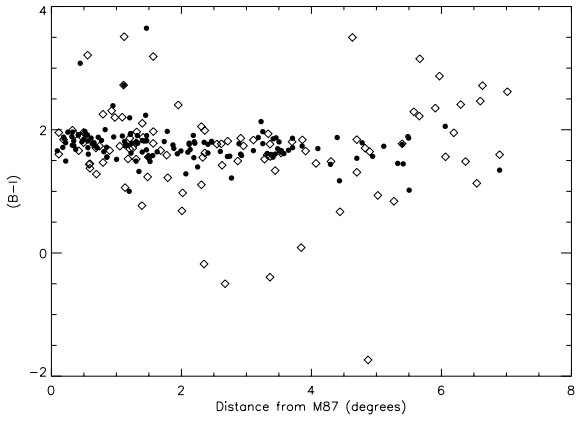

Figure 3. $B-I$ colours plotted as function of distance from M87, assumed as the centre of the cluster. Different symbols refer to different morphological types: filled circles for dE and diamonds for dI and VLSB. The sample does not seem to have any dependence upon distance from the cluster centre. Average error on the $(B-I)$ colour value is 0.25. Points which deviate more from the mean value have larger errors, as shown in Fig. 5.

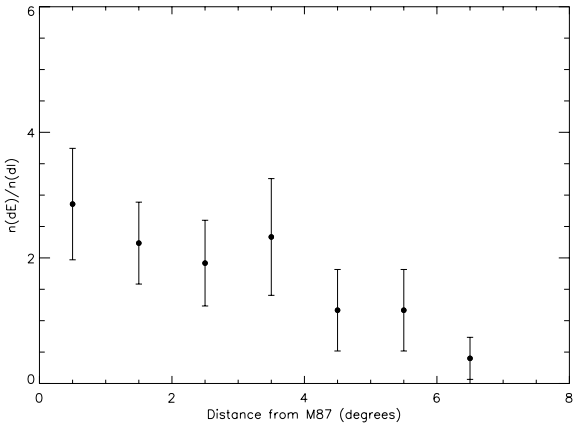

Figure 4. dE-to-dI ratio as a function of cluster-centric distance.

the centre of the cluster, the numerical ratio of dEs to dIs (Fig. 4) shows a morphology–density relation. This, we believe, could be an important clue to the nature of the cluster dwarf galaxy population: the well-ordered spherically symmetric galaxies (dE) are preferentially found towards the cluster centre, the more irregular galaxies (dI) towards the cluster edge. This is directly analogous to the bright galaxy morphology–density relation (Dressler 1984). In the same way as it has been proposed that spiral galaxies are being transformed into S0 galaxies in the cluster environment (Kodama & Smail 2001, and references therein) this could indicate that infalling dI galaxies are transformed into dEs (Davies & Phillipps 1989; Conselice et al. 2003a).

Figs 5 and 6 show the distribution of colours as a function of total absolute magnitude and central surface brightness, respectively. Again, the distributions do not show any correlation. Fig. 5 clearly shows that the scatter in colours has a dependence on total magnitude. In this figure we also give an estimate of the average error at each magnitude. The errors on the colours were calculated considering the following two independent contributions: (1) a systematic error owing to the aperture photometry procedure; and (2) the error in the calculation of the sky subtraction, which depends on the area of the object. Although the errors on the colour increase at the fainter magnitudes, the scatter is still much larger than the calculated errors. Fig. 7 shows that dE galaxies also have a narrower range of colours across the whole magnitude range [$(B-I)_{\rm median} = 1.8$; $\sigma = 0.3$],

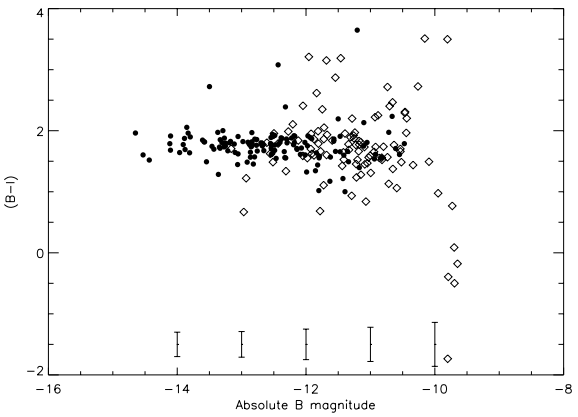

Figure 5. $B-I$ colours plotted as function of total B absolute magnitude. The average errors on the $(B-I)$ colour value as a function of the total B magnitude are shown.

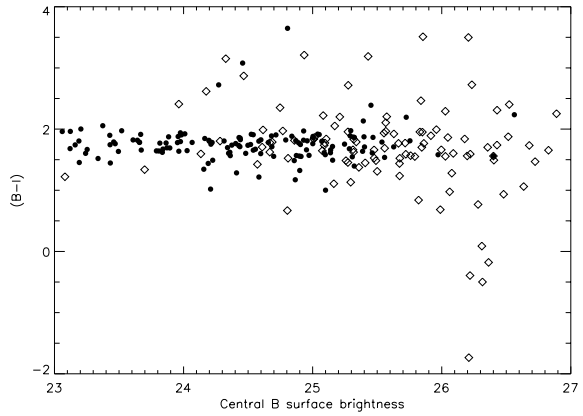

Figure 6. $B-I$ colours plotted as function of central B surface brightness.The colours appear to be spread out along the range of magnitudes considered without any evident correlation, although it has to be noticed that the extremely blue colours are found for $\mu_0 < 1\sigma_{\rm sky}$ ($\sim$26 B mag arcsec^{-2}). Average error on the $(B-I)$ colour value is 0.25. Points with large deviation from the mean value have larger errors, as shown in Fig. 5.

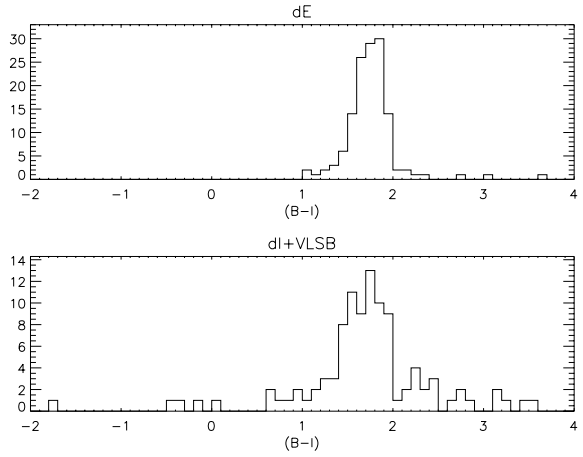

Figure 7. $(B-I)$ colour distribution for dE and dI, respectively. Median and standard deviation values for the two distributions are respectively: $(B-I)_{\rm dE} = 1.8$, $\sigma_{\rm dE} = 0.3$; $(B-I)_{\rm dI} = 1.7$, $\sigma_{\rm dI} = 0.7$.

while dI galaxies have a much broader range [$(B-I)_{\rm median} = 1.7$; $\sigma = 0.70$] possibly indicating their different evolutionary states i.e. undergoing, fading from or between a burst of star formation. For comparison, Karick, Drinkwater & Gregg (2003) also find a wide range of colours for their Fornax Cluster dwarf galaxies, larger than that of brighter galaxies.

5.1 Comparison with synthetic colours

For comparison with our colour distribution, in Fig. 8 we show the $(B-I)$ colour predictions obtained using the PEGASE evolutionary synthesis code (Fioc & Rocca-Volmerange 1997). The figure shows $(B-I)$ as a function of time and different points for each age refer to different initial metallicities and SFRs chosen in the simulation. Aware that one colour is not enough for disentangling the effects of metallicity and age (i.e. the age–metallicity degeneracy; Worthey 1994, and references therein), we did not explore the synthesis code in all its potentialities and we run it instead, using the default choices for the many permitted parameters: a Salpeter initial mass function (with lower mass 0.1 $M_\odot$ and upper mass 120 $M_\odot$), a range of

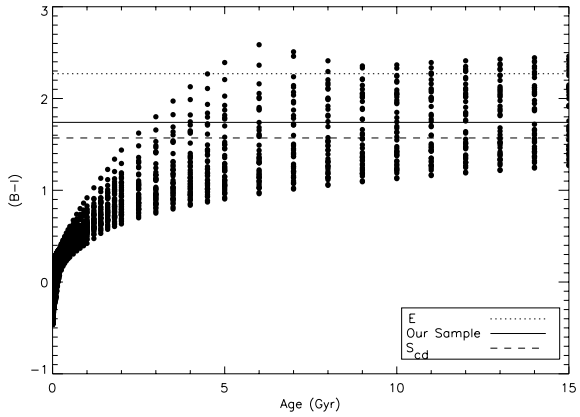

Figure 8. Synthetic $(B - I)$ colours as function of time produced using the PEGASE evolutionary synthesis code. Overlayed in the plot, as explained in the legend, are the median $(B - I)$ colour of our distribution (filled line) and for comparison a typical value for an elliptical galaxy (dotted line) and for a late-type spiral (dashed line). These latter values are taken from Fukugita, Shimasaku & Ichikawa (1995).

metallicities (0.1, 0.05, 0.02, 0.008, 0.004, 0.0004, 0.0001 $Z_{\odot}$) and different exponential SFRs with decay times 1, 2, 4, 8, 16 and 32 Gyr.

The main intention with this comparison is to show that the distribution of galaxy colours of our sample lies well in the average range of the expected values from synthetic models (Fig. 8, filled line) . Also, some of our extremely blue colours are compatible with very young ages, but one colour is not enough to claim any definitive conclusion and, as we have shown, errors on these extremely blue colours are quite large. As a comparison, average values for an elliptical galaxy and a late-type spiral (Fukugita et al. 1995) have been overlayed in the plot of Fig. 8. It is interesting that the average colour of the dwarfs in our sample is closer to that of a spiral and bluer than that of an elliptical, suggesting that these dwarfs have possibly consumed their gas until recent epochs. However, Fig. 8 clearly shows that it is not possible to obtain conclusive results from this analysis with one colour only; combined observations in a third band (e.g. the K band) would help disentangling the age–metallicity degeneracy. We will be doing this as part of the near-infrared survey UKIDSS (UKIRT Infrared Deep Sky Survey) – see, www.ukidss.org. In the following sections, however, as a working hypothesis, we will assume that the galaxies in our sample have similar metallicity so that the relative $B - I$ colour differences are indicative of differences in age.

5.2 Comparison with different environments of the Local Universe

Although it is in principle difficult to combine results from samples selected in different ways, in Fig. 9 we plot the distribution of the $(B - I)$ colours of galaxies from our sample and for comparison the same distributions for dwarf galaxies in different environments of the nearby universe: the field (Makarova 1999); the Ursa Major Cluster (Trentham, Tully & Verheijen 2001); the Virgo Cluster (from our catalogue); and the Fornax Cluster (Karick et al. 2003). Table 1 gives the median and standard deviation for these distributions, along with some relevant properties of the environments.

Table 1 and Fig. 9 suggest that the average colour distribution of dwarf galaxies becomes progressively redder, when proceeding from the field to denser, more elliptical galaxy-dominated environments. Gallagher & Hunter (1984) found the same trend comparing

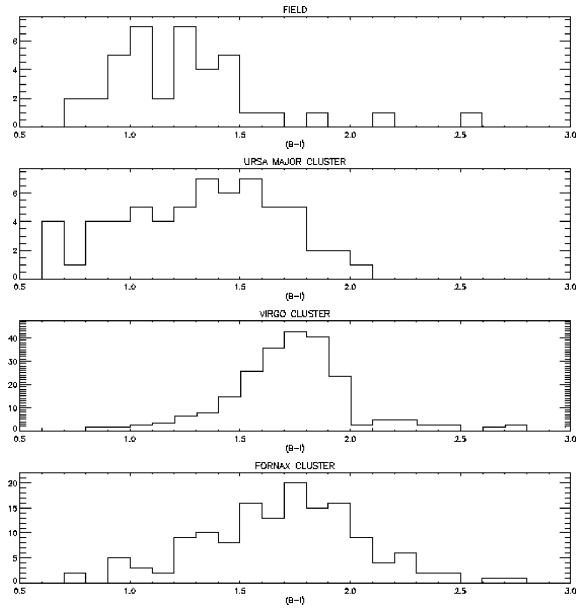

Figure 9. $B - I$ colour distribution of dwarf galaxies in different environments, from top to bottom: the field, the Ursa Major, the Virgo and the Fornax Clusters.

Table 1. Median and standard deviation for dwarf galaxies $B - I$ colours distribution in different environments for comparison with our results in the Virgo Cluster. We also list some of the possibly relevant properties of the environments.

Environment	Mass (10^{14} $M_{\odot}$)	Crossing time (H_0^{-1})	$(B - I)_{\rm median}$	Standard deviation
Nearby (field)	–	–	1.2	0.3
Ursa Major	0.5	0.5	1.4	0.4
Virgo	8.9	0.1	1.7	0.5
Fornax	0.7	0.1	1.8	0.2

dI of the Virgo Cluster to a field sample. Although the nature of the dwarfs considered in the samples of Fig. 9 might be different (ours being very faint), this result seems to indicate a strong environmental effect on the stellar population of these galaxies: the cluster environment progressively affects the evolution of dwarf and giant galaxies in the same way. Whether this is owing to a progressively enhanced SFR in denser environments or to stronger gas stripping that stopped SF earlier, leaving the cluster with an old galaxy population, needs further investigation on the exact nature of the stellar population of these dwarfs galaxies. A more detailed discussion concerning these points is deferred to Section 7.

6 H I OBSERVATIONS

The H I data are 21-cm H I line pointed observations with the 305-m Arecibo telescope of a subsample of galaxies from our catalogue. Many H I surveys have been made of, or in, the Virgo Cluster area, aimed at detecting dwarf galaxies (Hoffman et al. 1985, 1989; Conselice et al. 2003a). A blind H I line survey of the entire cluster, providing a comprehensive census of gas-rich objects, has recently been carried out by the HIPASS team, but the data are, as yet, unavailable. Davies et al. (2004) have carried out a deep blind Jodrell Bank survey of a 4×8 deg region in the Virgo Cluster. The results from this survey indicate a relative lack of low-mass H I objects

compared, to the field: galaxies in the cluster environment are depleted in gas compared to field galaxies – either through the gas-loss mechanisms or through accelerated star formation. This survey has also, surprisingly, shown the presence of two objects without optical counter parts (Davies et al. 2004). Although a further investigation is required to confirm these objects, this result shows how H I observations can still provide new and interesting results in the Virgo Cluster.

The 3σ H I mass detection limit for a typical $75\,\mathrm{km\,s^{-1}}$ wide flat-topped dwarf profile for the Davies et al. blind survey is about $10^8\,\mathrm{M_\odot}$, corresponding to a gas-rich ($(M_{\mathrm{H\,I}}/L_B)_\odot \sim 1$) dwarf of absolute magnitude $M_B \sim -14.5$ at $d = 16$ Mpc. This is the typical value of the brightest dwarfs in our sample. With its extraordinary sensitivity the Arecibo telescope offers the opportunity to go deeper on specific targets and easily reach typical H I mass detection limits at the Virgo Cluster distance of an order of magnitude smaller (see Section 6.3.2).

The general gas deficiency of Virgo Cluster members is a well-established phenomenon (Solanes et al. 2002 and references therein; Davies et al. 2004). Deep H I pointed observations of 59 Virgo Cluster dEs from the VCC by Conselice et al. (2003a) yielded only seven clear detections (just two of which are new) for objects having a mean blue absolute magnitude M_B of -16 (range: -14.2 to -17.0) and with an average $M_{\mathrm{H\,I}} = 2.5 \pm 3.6\,10^8\,\mathrm{M_\odot}$, $(M_{\mathrm{H\,I}}/L_B)_\odot = 0.57 \pm 0.52$ and full width at half maximum (FWHM) linewidth $W_{50} = 125 \pm 93\,\mathrm{km\,s^{-1}}$. Even if the expected detection rate was low, we carried out H I follow ups of a subsample of our galaxies, because dwarf galaxies in clusters do include star-forming, and generally H I-rich, dwarf irregulars (e.g. Gallagher & Hunter 1984) as well as quiescent, gas-poor dwarf elliptical/spheroidals (e.g. Ferguson & Binggeli 1994; Gallagher & Wyse 1994). H I observations are required for a clearer understanding of their nature, in order to confirm their cluster membership, place lower limits on the H I mass of the non-detected objects, obtain $M_{\mathrm{H\,I}}/L_B$ ratios or upper limits and look for environmental effects on their gas content.

6.1 Sample description

From our catalogue of 231 candidate LSB dwarf members of the Virgo Cluster, we observed 100 objects in H I according to the following priorities during the observing run: we first selected objects that were not part of the VCC catalogue, that did not lie within 1 deg from the strong continuum source M87 (see Section 6.2) and we gave priority to dI or VLSB morphological types. The galaxies observed at Arecibo are listed in Table 2 if detected in H I along with their global optical and H I properties, while a small sample of the non-detections is listed in Table 3 (a full version of Table 3 can be found online at http://www.blackwellpublishing.com/products/journals/suppmat/mnr/mnr8608/mnr8608sm.htm). The galaxies are given a name from our catalogue and a name from the literature, if previously catalogued; the cross-correlation with other catalogues

Table 2. Objects detected in H I at Arecibo. Column 1, the number of the object from our catalogue; column 2, identification from other catalogues (T, Trentham & Hodgkin 2002; U, UGC); column 3, right ascension (J2000.0); column 4, declination (J2000.0); column 5, morphological type; column 6, total apparent blue magnitude; column 7, central blue surface brightness; column 8, disc scalelength; column 9, $B-I$; column 10, rms noise level of the H I spectrum; column 11, integrated H I line flux; column 12, H I profile width at 50 per cent of peak maximum; column 13, same at 20 per cent; column 14, H I line centre velocity; column 15, distance; column 16, H I mass; and column 17, H I mass to blue luminosity ratio.

Obj.	Ident	RA (J2000.0)	Dec. (J2000.0)	T	m_{B_T} (mag)	$\mu_{0,B}$	α_B (arcsec)	$B-I$	rms (mJy)	$I_{\mathrm{H\,I}}$ (Jy km s^{-1})	W_{50} (km s^{-1})	W_{20} (km s^{-1})	$V_{\mathrm{H\,I}}$ (km s^{-1})	d (Mpc)	$M_{\mathrm{H\,I}}$ (10^8 M$_\odot$)	$M_{\mathrm{H\,I}}/L_B$ (M$_\odot$/L$_{\odot,B}$)
144		123841	115843	dI	19.8	26.6	9	–	0.8	0.47	77	125	1036	16	0.3	6.2
158	TH152	125107	120339	dI	17.1	23.3	7	1.21	0.9	1.71	63	83	1788	16	1.0	1.7
249	U8061	125644	115557	dI	17.0	23.7	9	1.46	1.5	2.12	69	89	563	16	1.3	1.9
4	TH225	124112	105601		17.7	23.6	6	1.37	0.9	1.13	175	125	6468	85.5	19.8	2.0
27		124934	121411		18.2	23.3	4	1.24	1.0	1.03	197	297	7146	94.7	22.0	3.1

Table 3. Objects not detected in H I at Arecibo. [1] Number from our catalogue, [2] identification from other catalogues, [3] right ascension (J2000.0), [4] declination (J2000.0), [5] morphological type, [6] total apparent blue magnitude, [7] central blue surface brightness, [8] disc scalelength, [9] rms noise level of H I spectrum, [10] estimated 3σ upper limit to the integrated H I line flux, for assumed 75 km s^{-1} wide flat-topped profiles, [11] estimated upper limit to the H I mass, at the assumed 16 Mpc distance of the Virgo Cluster and [12] estimated upper limit to the H I mass to blue luminosity ratio. This is a sample of the full table, which is available online at http://www.blackwellpublishing.com/products/journals/suppmat/mnr/mnr8608/mnr8608sm.htm

Obj.	Ident	RA (J2000.0)	Dec. (J2000.0)	T	m_{B_T} (mag)	$\mu_{0,B}$	α_B (arcsec)	$B-I$	rms (mJy)	$I_{\mathrm{H\,I}}$ (Jy km s^{-1})	$M_{\mathrm{H\,I}}$ (10^7 M$_\odot$)	$M_{\mathrm{H\,I}}/L_B$ (M$_\odot$/L$_{\odot,B}$)
Mhi M/Lb <1.2												
0		123215	105622	dI	20.2	26.4	7	1.6	1.1	<0.3	<1.7	<5.2
1		123333	110528	dE	19.8	24.8	4	3.6				
2		124032	111021	dI	21.3	26.3	4	−0.5	1.0	<0.2	<1.4	
3		124130	111245	dI	20.9	26.4	5	1.5	0.8	<0.2	<1.2	<7.3
5		124843	105641	dE	18.1	23.1	4	1.2	0.9	<0.2	<1.4	<0.6
6	VCC2062	124800	105816	dI	18.0	24.8	9	0.7				
7		123233	111508	dE	18.5	24.0	5	1.9	1.3	<0.3	<2.0	<1.3
8		123250	112515	dI	20.6	25.6	4	2.2				
10		123808	111725	dE,N	18.5	23.5	4	1.6	1.2	<0.3	<1.8	<1.1
11		123729	111900	vlsb	20.3	26.5	7	2.4	0.9	<0.2	<1.4	<4.8

was made within a 15-arcsec radius search area around our optical centre positions.

In addition, included in our observations are 15 LSB objects listed in the literature (Trentham & Hodgkin 2002; VCC) as candidate Virgo Cluster members, that are located in the east–west strip, but were not picked out by our detection algorithm (for discussion on this point see paper I). We observed these 15 sources in H I as most were classified as dI and therefore are potentially H I gas rich.

6.2 Data reduction

Data were taken with the *L*-band narrow receiver using nine-level sampling with two of the 2048 lag subcorrelators set to each polarization channel. All observations were taken using the position-switching technique, with the blank sky (or OFF) observation taken for the same length of time, and over the same portion of the Arecibo dish as used for the on-source (ON) observation. Each 3 min+3 min ON+OFF pair was followed by a 10-s ON+OFF observation of a well-calibrated noise diode. The overlaps between both subcorrelators with the same polarization allowed a wide velocity search while ensuring an adequately coverage in velocity. The velocity search range was -1000 to 11 000 km s^{-1}, as the Virgo Cluster extends from 500 to 2500 km s^{-1} (Binggeli et al. 1993). The HPBW of the instrument at 21 cm is 3.6 arcsec × 3.5 arcsec and the pointing accuracy is about 15 arcsec.

A filter was used to cut off all emissions at frequencies below 1371 MHz, thus eliminating radio frequency interference (RFI) from radars on Puerto Rico. The strongest RFI signal noted was centred on 1381 MHz (or 8300 km s^{-1}), which, however, did not occur frequently.

Using standard Interactive Data Language data-reduction software available at Arecibo, corrections were applied for the variations in the gain and system temperature with zenith angle and azimuth, a baseline of order one to three was fitted to the data, excluding those velocity ranges with H I line emission or RFI, the velocities were corrected to the heliocentric system (using the optical convention) and the polarizations were averaged. All data were boxcar smoothed to a velocity resolution of 15 km s^{-1} for further analysis. For all smoothed spectra the rms noise level was determined and for the detected lines the central velocity, linewidths at, respectively, the 50 per cent and 20 per cent level of peak maximum, and the integrated flux were determined.

The extremely strong continuum emission from M87 aversely affected the rms noise level and the quality of the baselines in a sizeable area ($\sim 1^\circ$) surrounding it. M87 is a 220-Jy source at 1415 MHz, with a core and two lobes extending some 15 arcmin from the core. Attempts were made to correct the bandpass by applying a double-switching technique in which an ON+OFF spectrum of a target galaxy is normalized with an ON+OFF spectrum of the continuum source influencing the data, i.e. M87, taken just after. Although this technique has been applied successfully at Arecibo to H I data of galaxies with continuum sources (e.g. Ghosh & Salter 2002), the situation near M87 is fundamentally different as it is detected through the far side-lobes of the telescope, rather than through the main beam, and it is strong enough to cause non-linear saturation effects in the receiver system. As we could not obtain proper quality data within about 1 deg from M87, we stopped observing objects in that area (see Fig. 1).

6.3 Results

Out of the 115 objects we observed in H I just five were detected, three of which are members (i.e. have line centre velocities in the range 500–2500 km s^{-1}). Optical *B*-band images from our deep CCD frames and H I spectra of these sources are shown in Fig. 10 and a discussion on individual objects is given in next section. Table 2 gives their global optical properties measured in the *B* band as well as the integrated line fluxes of the detections: $I_{\rm H\,I}$, the W_{50} and W_{20} linewidths, the centre velocities $V_{\rm H\,I}$, the total H I mass $M_{\rm H\,I}$ and the H I mass-to-light ratio $M_{\rm H\,I}/L_B$. The total H I mass, given in $M_\odot$, is derived from the total flux according to the following formula:

$$M_{\rm H\,I} = 2.365 \times 10^5 \times D^2 \int S(v)\,{\rm d}v, \qquad (2)$$

where the distance D is given in Mpc, the flux $S(v)$ in Jy and the velocity v in km s^{-1} (Roberts 1968).

All the given radial velocities are heliocentric and expressed according to the conventional optical definition [$V = c(\lambda - \lambda_0)/\lambda_0$]. For objects with radial velocities that lie inside the range occupied by Virgo Cluster members, ~ -500 to 2500 km s^{-1}, a distance d of 16 Mpc was assumed. For other objects distances were calculated using radial H I velocities corrected to the Galactic Standard of Rest, following the procedure given in the Third Reference Catalogue of Bright Galaxies, and assuming a Hubble constant of $H_0 = 75$ km s^{-1} Mpc^{-1}.

6.3.1 Notes on individual objects

144: this object is a cluster member, which we detected at $V_{\rm H\,I} = 1036$ km s^{-1}. Its projected distance from the cluster centre is $\sim 2^\circ$. Its extremely low central surface brightness (26.6 *B* mag arcsec^{-2}) makes it almost impossible to see on the *B* band image. With an H I mass-to-light ratio of 6.2, it is an extreme case of either a very young galaxy or a galaxy where the conversion of gas into stars has been very inefficient. The $(B - I)$ colour for this galaxy is not available, because the noise in the *i*-band image is too high to measure its flux.

158 (= T152): this object is a cluster member at a cluster-centric distance of $\sim 5^\circ$, which we detected at $V_{\rm H\,I} = 1788$ km s^{-1}. It is an irregularly shaped galaxy with several clumps in the *B* band image.

249 (= UGC 8061): this object is an irregular LSB VCC galaxy at cluster-centric distance of $\sim 6.5^\circ$. Although our centre velocity and line flux are in agreement with those of Schombert, Pildis & Eder (1997) and Huchtmeier et al. (2000), who found $V_{\rm H\,I} = 562$ km s^{-1} and $I_{\rm H\,I} = 2.0$ Jy km s^{-1}, our W_{50} of 72 km s^{-1} is larger than their 55 km s^{-1}. The *B*-band image shows a very irregular galaxy with several clumps surrounded by diffuse light.

4 (= T225): this object, also classified as dI by Trentham & Hodgkin (2002), is a background galaxy, which we detected at $V_{\rm H\,I} = 6468$ km s^{-1}. Its W_{50} linewidth of 174 km s^{-1} is much larger than what is usually found for dwarf galaxies. It could resemble the extreme late-type field galaxies discussed by Matthews & Gallagher (1997) in terms of its optical structure and H I line profile.

27: this edge-on object is a background galaxy, which we dete cted at $V_{\rm H\,I} = 7146$ km s^{-1}.

6.3.2 Notes on non-detections

The average noise for our spectra is ~ 1 mJy at a velocity resolution of 15 km s^{-1}. Assuming a typical FWHM for the H I profile of the dwarfs to be 75 km s^{-1} and a 3σ detection threshold, at a distance of 16 Mpc, the non-detections have an average upper mass limit of $\sim 1.5 \times 10^7\,M_\odot$ which translates into a column density limit of $\sim 5 \times 10^{18}$ atom cm^{-2} (assuming a limiting mass galaxy filling the beam at the cluster distance).

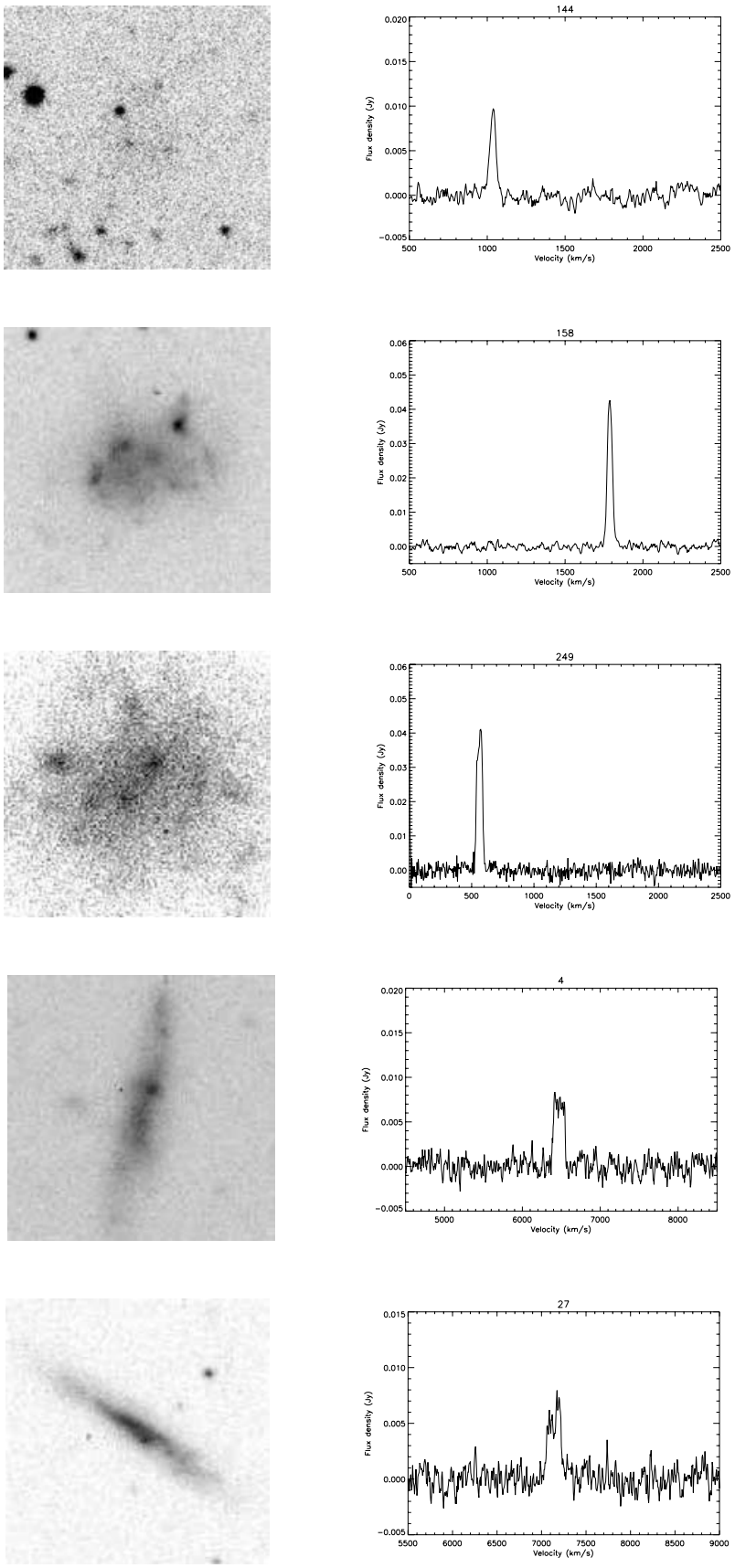

Figure 10. *B*-band images and H I spectra for the five non-confused H I detections; respectively numbers 144, 158, 249, 4 and 27 from our catalogue.

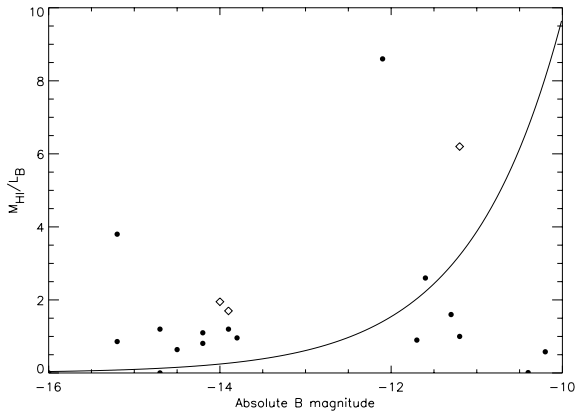

Figure 11. $M_{\rm HI}/L_B$ 3σ detection limit for our survey as a function of absolute B magnitude of Virgo Cluster dwarf the galaxies, for an assumed $75\,{\rm km\,s^{-1}}$ linewidth. Dots in the plot are dwarf galaxies from the Local Group that have H I emission (Mateo 1998); diamonds are our detections.

The estimated upper limits of the $(M_{\rm HI}/L_B)_{\odot}$ ratio range from 0.1 to 12, depending on the galaxy absolute magnitude. In Fig. 11 we show this detection limit as a function of absolute B magnitude (solid line): values of $M_{\rm HI}/L_B$ below the curve are not detectable in our H I observations. Diamonds in the figure are detections from our sample and dots are Local Group dwarf galaxies with measured H I (Mateo 1998): 62 per cent of these lie above our H I detection limit. If we consider only the ones that would satisfy our optical selection criteria at the Virgo distance, the expected detection rate in H I would still be 50 per cent, for galaxies with the same properties as the Local Group ones. This is considerably higher than the 4 per cent detection rate of the observations of our sample and is again a strong indication of how different the properties of dwarf galaxies in these two environments are. The plot also clearly shows that very faint galaxies need high $M_{\rm HI}/L_B$ values in order to be detected.

The H I content of dwarf galaxies in the Local Group clearly distinguishes them as dI (that show H I emission) and dSph/dE that mostly do not have any detectable H I emission (Mateo 1998). Regardless of their morphological type our results are consistent (even if not conclusive) with the idea that the gas in these galaxies has been either stripped away or efficiently converted into stars. The results from the H I observations are also consistent with those for the average value of the $B-I$ colours: on average, the galaxies in our sample do not show signatures of a young stellar population, suggesting that the cluster environment has accelerated their evolution.

A pilot sample of LSB dwarf galaxies identified in the Millennium Galaxy Strip (MGS) was also observed during this Arecibo run. As already pointed out, this is a data set in the field that is identical to ours in the Virgo Cluster and the same detection algorithm was applied to it, to obtain a catalogue of dwarf LSB galaxies (Roberts et al. 2004). The H I detection rate for this pilot sample is considerably higher than for our sample in the Virgo Cluster: four out of the 14 (∼30 per cent) observed MGS field galaxies show H I emission, compared to five out of 115 (∼4 per cent) in the cluster. Consistent with the well-estabilished trend for clusters to host gas-poor dwarfs, this result confirms the importance of the role played by the environment in the evolution of the gas content of dwarf galaxies.

As a last remark, our H I observations of the Virgo Cluster sample rule out the possibility that our catalogue is highly contaminated by gas-rich background or foreground galaxies – this being one of the main worries when discussing the faint-end slope of the LF of a cluster or its dwarf galaxy content. According to our observations, the non-detections are also non-background/foreground (H I-rich) galaxies in the velocity range of -1000 to $11\,000\,{\rm km\,s^{-1}}$.

7 DISCUSSION

Before discussing our results, let us summarize them for clarity.

(i) There are cluster dE galaxies that have a small range of colours that are preferentially found towards the centre of the cluster and are gas poor. Dwarf ellipticals are usually passively evolving (no or little star formation) galaxies and the average colours that we found are consistent with this picture and possibly indicative of an older stellar population.

(ii) There are cluster dI galaxies that have a wider range of colours which tend to reside in the outskirts of the cluster. They appear to have star formation regions and the wide range of colours may reflect different current star formation states.

(iii) There seems to be an environmental dependency of the $B-I$ colour distribution of dwarf galaxies in the Local Universe.

(iv) There are about five times as many dwarf galaxies ($-14 < M_B < -10$) per giant galaxy ($M_B < -19$) in the Virgo Cluster than in the general field and in the Local Group (paper I). A considerable part of these galaxies seem to constitute a cluster dwarf population rather than being associated with the giants. In addition, the number of dwarfs possibly associated with giant galaxies in Virgo (i.e. their projected distance is within the giant tidal radius) is on average ∼13, compared with ∼4 for the Local Group. Because of this excess of dwarfs, the cluster cannot have been simply constructed by infalling small groups like the Local Group.

(v) On the whole, the cluster dwarf galaxy population is gas poor compared to the dwarf galaxies in the Local Group and in the field.

(vi) The LF of the cluster over the range ($-14 < M_B < -10$) is steeper than that in the field. In addition, distinguishing inner and outer regions for the cluster, the LF in the former region is flatter than in the latter (paper I).

(vii) The H I mass function of the cluster appears to be less steep than the H I mass function of the field. Combining this with the observed steep LF leads suggests that, in the cluster, gas has been more efficiently converted into stars (Davies et al. 2004); stripping mechanisms might also, however, produce this result.

(viii) In addition, Conselice et al. (2003a) have shown that the Virgo Cluster dE population is dynamically similar to the spiral rather than the elliptical galaxy population. They argue that this implies that the dE population is not primordial; rather it is a population that has fallen into the cluster at a later date.

In the following sections we discuss possible physical processes acting on the dwarf galaxies in the cluster environment and the influence that they have on the results described above. In particular there have been numerous attempts in the past to look for mechanisms that remove gas from cluster dwarf galaxies to explain their red colours (no recent star formation) and their lack of gas. Contrary to this, we believe that our results can be explained by accelerated star formation that consumes the galaxy gas, rather than gas-stripping mechanisms (see Section 7.4).

Part of the analysis that follows is similar to that extensively and comprehensively discussed in a series of papers by Conselice, Gallagher & Wyse (2001); Conselice (2002); Conselice et al. (2003a); Conselice, Gallagher & Wyse (2003b). We formulate the

problem in a slightly different way, concentrating on the mass-to-light ratios required to avoid gas stripping (see also Davies & Phillipps 1989). Dwarf galaxies may in fact be very robust objects in the intergalactic medium. For example the recent work by Kleyna et al. (2002) on the velocity dispersion of stars in the outskirts of the Local Group galaxy Draco has revised its mass-to-light (M/L) ratio from about 100 to 440.

7.1 Ram-pressure stripping

A cluster like Virgo has a substantial ICM which is detected via its X-ray emission (Vollmer et al. 2001). A galaxy moving through the ICM is subject to a ram pressure that can possibly strip its gas away, if the ICM pressure on the galaxy is stronger than its internal gravitational force (Gunn & Gott 1972). Ram pressure stripping has often been used in order to explain the H I deficiency of galaxies in clusters compared with galaxies in the field (Chamaraux, Balkowski & Gerard 1980; van Gorkom 2003; Lee, McCall & Richer 2003).

Following Davies & Phillipps (1989), we can set a limit for the dynamical mass-to-light ratio $M_{\rm dyn}/L_B$ that a galaxy requires to survive the ram-pressure stripping

$$\left(\frac{M_{\rm dyn}}{L_B}\right) > \rho_0 \left(1+\frac{r^2}{r_c^2}\right)^{-(3/2)\beta} \frac{v_\perp^2}{\sigma_{\rm gal}} \times 10^{0.4(\Sigma-26.8)}, \qquad (3)$$

where $v_\perp$ is the orthogonal velocity of the galaxy through the ICM (km s^{-1}), $\sigma_{\rm gal}$ is the gas surface density in the galaxy (M$_\odot$ pc^{-2}), Σ is the average surface brightness of the galaxy (B mag arcsec^{-2}) and the density of the ICM (atom cm^{-3}) is a function of position in the cluster and was parametrized according to a β model (Cavaliere & Fusco-Femiano 1976). For the Virgo Cluster $\beta = 0.45$, $\rho_0 = 4 \times 10^{-2}$ cm^{-3} and $r_c = 13.4$ kpc (Vollmer et al. 2001). Also, assuming $v_\perp = 700$ km s^{-1} (i.e. the average velocity dispersion of dwarfs in the Virgo Cluster) and $\sigma_{\rm gal} = 5$ M$_\odot$ pc^{-2} ($= 5 \times 10^{20}$ atom cm^{-2}, i.e. an average value for dwarf galaxies; Blitz & Robishaw 2000), we obtain limits for the mass-to-light ratio for different central surface brightness values of galaxies as a function of distance from the cluster centre. We take Σ to be the mean surface brightness over the half light radius ($\Sigma = \mu_{0,B} + 1.15$). We plot these curves in Fig. 12: different colours refer to different central surface brightness. For each curve and each colour, only galaxies above the curve are not affected by the ram-pressure stripping and retain their gas. The open diamonds in the plot show the galaxies in our sample with H I detection and the dots indicate the non-detections (see Section 6).

For galaxies without H I detection the M/L ratio was calculated using a dark matter halo ($M_{\rm h}$) to baryonic ($M_{\rm b}$) mass given in Persic, Salucci & Stel (1996). Note that this formula may severely underestimate the M/L ratio (Kleyna et al. 2002).

For the three galaxies with H I detection, the M/L ratio was calculated making use of the measured velocity width as follows:

$$M_{\rm dyn} \geqslant V_{\rm rot}^2 R_{\rm opt}/G \qquad (4)$$

and assuming the rotational velocity $V_{\rm rot}$ of the galaxy to be half of W_{50}, and the optical radius $R_{\rm opt}$ to be two disc scale lengths (h)

$$M_{\rm dyn} \geqslant 0.5 W_{50}^2 h. \qquad (5)$$

Note that the values obtained in this way are actually lower limits, as the H I radius is usually larger than the optical one. Our calculated values for the three galaxies with H I detections lie above the corresponding $M_{\rm dyn}/L_B$ limit for the occurrence of ram-pressure stripping.

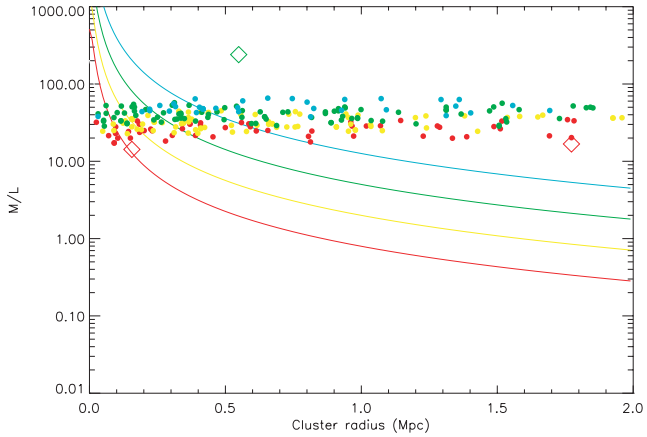

Figure 12. Curves of the M/L_B ratio limit for ram-pressure stripping to occur, as a function of distance from the centre of the cluster. Galaxies with M/L_B above the curves are able to retain their gas, having a gravitational force stronger than the ram pressure of the ICM. Different colours refer to different average surface brightness values in equation (3): red for $\mu_0 = 24$; yellow for $\mu_0 = 25$; green for $\mu_0 = 26$, blue for has $\mu_0 = 27$. Dots are all the galaxies from our sample and open diamonds are the three cluster galaxies that have been detected in H I. The colour of the dots are related to the galaxy average surface brightness according to the colours of the lines.

According to the lines of different surface brightness in Fig. 12, we can see that the majority of galaxies are not likely to be currently affected by ram-pressure stripping. In fact, regardless of their central surface brightness, the plot shows that galaxies are subject to stripping only if they lie within the core radius of the cluster, which corresponds to $R_{\rm c} = 0.5$ Mpc for the Virgo Cluster. This is in agreement with the observed gas deficiency of bright galaxies in the centre of the cluster (see, for example, Solanes et al. 2001, for spiral galaxies in the Virgo Cluster). Note that the cluster gas density falls rapidly to 2.8×10^{-4} cm^{-3} at the core radius of 0.5 Mpc – thus over most of the cluster the gas density is much lower than that assumed in ram-pressure stripping simulations (Marcolini, Brighenit & Ercole 2003). We should also take into account that the positions plotted for our galaxies are projected ones: galaxies at a small projected distance to the centre may actually lie in the outskirts of the cluster. The actual distance of such a galaxy would then be larger and the point representing it would move to the right in our plot, thus increasing the number of dwarfs that are not affected by ram-pressure stripping.

In fact, it is possible that none of our detected dwarfs are actually in the cluster core at all. Dwarf galaxies within the core are subject to tidal forces that could pull them apart. We can estimate the minimum size ($r_{\rm min}$) of a dwarf galaxy that would not be tidally disrupted at the cluster core (that is the distance at which the tidal stress is maximum; Merritt 1984), using the definition of the Roche limit

$$r_{\rm min} = R_{\rm c} \left(\frac{M_{\rm dwarf}}{3M_{\rm cluster}}\right)^{1/3} \qquad (6)$$

where $R_{\rm c}$ is the cluster core radius (0.5 Mpc; Binggeli et al. 1987), $M_{\rm dwarf}$ is the mass of the dwarf ($\approx 10^7$ M$_\odot$) and $M_{\rm cluster}$ is the mass within the core radius ($\approx 10^{14}$ M$_\odot$). This leads to a size of order 3 kpc, very similar to the sizes of our dwarf galaxies (1 kpc $\approx$10 arcsec at the distance of the Virgo Cluster), see also Merritt (1984). Dwarf galaxies passing through the core will be severely

disrupted by tidal forces (cf. intracluster light, stars and planetary nebulae; Gregg & West 1998; Arnaboldi et al. 2002). Given that most of our galaxies in the projected core region are mainly spherical dEs (Fig. 4), we conclude that it is unlikely that they are actually in the core (see also Ichikawa et al. 1988; Carey et al. 1996; Secker et al. 1998; Adami et al. 2000; Oh & Lin 2000; Conselice et al. 2001; Gnedin 2003).

Dwarf galaxies are resilient in the cluster because they have high values of the M/L ratio, but the ICM ram pressure may be important in triggering starbursts. Numerical simulations carried out with smoothed-particle hydrodynamics (Abadi, Moore & Bower 1999; Schulz & Struck 2001) and with N-body codes (Vollmer et al. 2001) show that, for small inclination angles (nearly edge-on) the ram pressure leads to a temporary increase in the central gas surface density. This, in turn, may give rise to an episode of star formation. We will consider the gas consumption through induced starbursts in Section 7.4.

7.2 SNe-driven winds

In almost all CDM models, SN-driven winds play a crucial role in suppressing the formation of stars in small dark matter haloes (dwarf galaxies), as they could, in principle, completely blow away its gas. As stated in the introduction this cannot be the complete solution to the substructure problem, owing to the large numbers of dwarfs found in some, but not in other, environments.

For a SN-driven wind to expel the gas from a dwarf galaxy, the energy in the wind has to exceed the gravitational binding energy (Dekel & Silk 1986). Davies & Phillipps (1989) showed that these energies are about equal for a dwarf galaxy with a M/L ratio of 100, leading to some uncertainty in whether this is a viable method at all for removing gas from dwarf galaxies. Following Davies & Phillipps (1989), we can write this condition as

$$T_{\rm W} > 10^3 (M_{\rm dyn}/L) r^2 10^{0.4(26.8-\Sigma)} \quad (7)$$

where $T_{\rm W}$ is the wind temperature and r is the galaxy radius in kpc. For $\Sigma = 24.5\ B$ mag arcsec^{-2} and $r = 1$ kpc, $T_{\rm W} > 10^4 (M_{\rm dyn}/L)$ for gas stripping to occur. Dekel & Silk (1986) give the range of $T_{\rm W}$ as 6×10^4 to 6×10^5 (Davies & Phillipps 1989). This uncertainty is further compounded by the confining pressure of the ICM for cluster galaxies (Babul & Rees 1992) and supported by the recent evidence of the large value of the $M_{\rm dyn}/L$ for dwarf galaxies in the Local Group (Kleyna et al. 2002).

The above conclusion is also further supported by recent, more detailed simulations, by Mac Low & Ferrara (1999) who investigated starbursting dwarf galaxies with baryonic masses $M_{\rm b} = 10^6$–10^9 M$_\odot$ and supernova (SN) rates from one per 3×10^4 yr to one per 3×10^6 yr. They showed that the critical masses for which the whole gas content is blown away are very low ($\leqslant 10^6$ M$_\odot$): in almost all the cases, the starburst is not energetic enough and creates only holes in the regions surrounding the supernovae event. Note that the total baryonic (stellar + gas) mass that we expect for our galaxies lies within the range they investigated: the stellar masses for our galaxies are $\sim 1.6 \times 10^6$ to $\sim 6 \times 10^7$ M$_\odot$ (as their magnitude range is $M_B \approx -10$ to -14); our H I observations (see Section 6.3.2) indicate that they have H I masses below about 1.5×10^7 M$_\odot$. The SN rates explored by them are also consistent with the starbursts that we consider. These results, along with the observed high values of the M/L ratio, must give concern as to whether SN-driven winds are a viable gas-stripping mechanism (see also Mayer & Moore 2004).

7.3 Tidal interactions

Gravitational interactions can cause mergers, reshape the galaxy and its content or trigger starbursts. Contrary to ram-pressure stripping, numerical simulations show that they may be important even at large distances from the cluster centre and that the numerous high-speed encounters occurring in clusters can give rise to morphological transformations, i.e. disc systems into dwarf spheroidals and dEs (Moore et al. 1999; Moore 2003).

Tidal interactions in the cluster could have produced in the past instabilities that accelerated the star formation activity of the galaxies, resulting in the currently observed $B - I$ colours[3] and depletion of the atomic gas. This possibility is discussed in the following section.

The colour distributions in Fig. 9 and the dynamical timescales in Table 1 indicate a dependence of galaxy properties with the crossing time. The crossing time is related to the density of the cluster (not its total mass), with the most dense clusters having the shortest crossing time. This suggests that local interactions of galaxies have a large influence on their subsequent evolution. The importance of these interactions depends on the encounter rate, which is related to the number density (n) of galaxies in the specific environment considered, the interaction cross-section (ϱ), the velocity of the galaxy through the cluster (v) and the age of the cluster (t). Using a simple rate argument we can write the characteristic number of interactions per galaxy as

$$N \approx n \varrho v t. \quad (8)$$

If, for the sake of simplicity, we assume the cluster age to be the same for the different environments that we considered in Section 5.2, then we can calculate the relative number of encounters compared to that occurring in the Virgo Cluster as a function of n and σ_v ($=v/\sqrt{2}$) only, the cross section being the same. Using, for consistency, the information we need in equation (8) for the three clusters (the total number of galaxies, virial radius and velocity dispersion) given by Tully et al. (1996), we find that the number of encounters experienced by galaxies in the Virgo Cluster is three times lower than in Fornax and 20 times higher than in the Ursa Major Cluster.[4] If encounters promote star formation, this would have lead to an increased past star formation activity going from the Ursa Major to the Virgo and Fornax Clusters and could thus account for the reddening of the colour distribution.

The rate of interaction is obviously density dependent and the balance between the destruction versus production rates is delicate, as noted for example in the Coma Cluster by Adami et al. (2000). Conselice (2002) show that a steepening or a flattening of the faint-end-slope of the evolved LF in a cluster is function of the maximum number of tidal interactions experienced by the galaxies. These simulations show that there should be a density threshold above which destruction is more efficient than creation. This argument can also be easily used to interpret the difference in the inner and outer LFs of the Virgo Cluster that we showed in paper I. The dwarfs that now remain in the cluster would then be 'survivors' to this processes and they would have continued to form stars over a longer period than systems that were destroyed (for example in the cluster core).

To complete this picture, we can also investigate how likely it is that a dwarf galaxy will have an interaction with another cluster

[3] Here, again, we are assuming that all the galaxies in our sample have similar metallicity, so that redder colours means older stellar population.

[4] Note that introducing a dependence on the estimated cluster ages, does not alter this result.

galaxy capable of completely disrupting it and/or stripping its gas away. To estimate this we can calculate the interaction cross section, ϱ ($= \pi r_{\rm p}^2$, with $r_{\rm p}$ the impact parameter), as the square of the Roche limit distance, R

$$\varrho \approx R^2 \approx r^2 (3M_{\rm gal}/M_{\rm dwarf})^{2/3}, \quad (9)$$

where $M_{\rm gal}$ is the mass of the galaxy the dwarf is interacting with and r is the dwarf galaxy radius. For a given cluster the number of interactions depends only on the cross-section ϱ. It is straightforward to show that a 10^{10} $M_\odot$ galaxy is about 45 times more likely to interact in this way with another 10^{10} $M_\odot$ galaxy than it is with a 10^7 $M_\odot$ dwarf galaxy. The reason is that the dwarf galaxy, owing to its small size has to be very close to the large galaxy ($\lesssim$10 kpc) for severe tidal disruption to occur (e.g. the Sagittarius dwarf galaxy of the Local Group). This would be a problem if most of the Virgo dwarf galaxy population were closely associated with the giant galaxy population. In Fig. 2, however, we have shown that there is a population of Virgo dwarf galaxies that is not associated with the giants. As we do not see large numbers of large galaxies undergoing disruptive tidal interactions we have to conclude that dwarf galaxy disruptive interactions are also uncommon. This also does not appear to be a viable method of gas loss.

If the cluster dwarf galaxy population originated from a tidally truncated population of larger field galaxies then their tidal radii should be of order $R_{\rm c}\sigma_{\rm dwarf}/\sigma_{\rm clust}$ where $\sigma_{\rm dwarf}$ ($\lesssim$10 km s^{-1}) and $\sigma_{\rm clust}$ ($\approx$700 km s^{-1}) are the dwarf galaxy and cluster velocity dispersion, respectively. The smallest calculated radius is of order the 7 kpc; this is larger than the dwarf galaxies in our sample ($\approx$1 kpc) implying that they must sit in much larger dark matter haloes. Moore et al. (1998) also give a prediction for values of the effective radii of harassed galaxies; these range from 5.3 to 1.6 kpc, again larger than the typical values for galaxies in our sample. This poses a problem to the harassment scenario as a means of producing the dwarf galaxies in our sample through morphological transformation of large discs. The transformation of infalling gas-rich (already small) dwarf irregulars, like those detected by us, is, however, still quite possible.

7.4 Gas loss through enhanced star formation

Direct evidence for galaxy evolution in clusters is given by the Butcher & Oemler effect (BOE; Butcher & Oemler 1978). Three triggering mechanisms have been suggested for the BOE: ram pressure by the hot ICM (Dressler & Gunn 1990); galaxy–galaxy interactions (Lavery & Henry 1988); and tidal triggering by the cluster potential (Henriksen & Byrd 1996). The lack of correlation of the BOE with X-ray luminosity, however, rules out the possibility that the former mechanism is the unique one at work. On the other hand, several studies of both statistical samples and individual interacting systems have shown that the optical and infrared colours of peculiar galaxies can be explained in terms of bursts of star formation triggered by tidal interactions (Larson & Tinsley 1978; Young et al. 1986; Larson 1986; Liu & Kennicutt 1995; Barton, Geller & Kenyon 2000, 2003). Theoretical work employing smoothed particle hydrodynamics (SPH) also gives support to the notion that galaxy interactions can drive significant inflows of gas under a wide range of conditions and rise the SFR by more than an order of magnitude (Noguchi & Ishibashi 1986; Barnes & Hernquist 1996; Mihos & Hernquist 1996).

Our view is that our observations can be explained not by gas-stripping mechanisms, as described above, but by accelerate star formation in infalling harassed dI galaxies or dark haloes that have no stars – the gas that once was there is still there, but now in the form of stars. This is witnessed by the very different cluster and field LF and H I mass function, the spatial distribution of dE and dI galaxies, their very different morphologies and gas content. We suggest that cluster dwarf galaxies have undergone accelerated evolution compared to the field.

Although we have shown that tidal interactions that strip a dwarf galaxy of its gas must be rare, numerical simulations do show that the several high-speed encounters that disc systems undergo in clusters can transform infalling galaxies into dEs. The continually varying tidal force compresses the gas, promoting enhanced star formation compared to dI galaxies in the field. As we have suggested in the previous section we believe that the galaxies that undergo this transformation are the gas-rich dIs observed on the cluster edge.

Can enhanced star formation alone explain the colour distribution of our galaxies and the possible lack of H I emission from the dwarfs of our sample? If we assume the initial H I mass of a dwarf to be 10^7 $M_\odot$ and that each tidal interaction triggers a starburst of $\sim 10^8$ yr duration and consumes $\sim 10^6$ $M_\odot$ of gas (Leitherer & Heckman 1995), then 10 such starbursts can fully exhaust the H I content of the dwarf.[5] This would make dwarfs in clusters very different from isolated dwarf irregulars that typically have long gas depletion timescales of $\sim$20 Gyr and which have experienced (and will continue to experience for at least another Hubble time) a slow, but constant, star formation activity (van Zee 2001).

What would happen to the colours and absolute magnitudes of the dwarfs in our simple model of several starbursts? Numerical simulations on the effects of starburst on LSB galaxies show that surface brightness is virtually unaltered by these episodes, while the total colours can change significantly (O'Neil, Bothun & Schombert 1998). According to Leitherer & Heckman (1995) the change in $(B - I)$ colour in 10^8 yr would be $\sim$1 mag, regardless of metallicities and for either continuous star formation activity or a single starburst. The colour distribution of our sample is consistent with such a scenario. The average $(B - I)$ colour of the galaxies is $\sim$1.7, which is about the typical colour for metal-poor globular clusters (Reed 1985). We should also note here that the three H I detections in our sample are extremely blue if compared with the average value of the colour distribution and with the colours of metal-poor globular clusters: 144 is not visible at all in the I band, 249 and 158 have $(B - I)$ colours of 1.46 and 1.21, respectively, indicating a younger population. These galaxies might then be interpreted as being part of an infalling population of initially gas-rich dIs that are possibly undergoing morphological transformations that will eventually turn them into gas-poor galaxies (see also Conselice et al. 2003a).

There are two further points to consider: the presence of intracluster light and planetary nebulae has been used to argue for the large-scale stripping of material from galaxies in the cluster. All of the above have only been detected within the Virgo Cluster core. We argued earlier that galaxies entering the core would be tidally disrupted and use this to suggest that our sample galaxies are not in the core, but their positions are projected on to it. Total tidal disruption is possible within the cluster core. Secondly, the observed luminosity–metallicity relation of dwarf galaxies has been used to argue that the more massive dwarfs retain their gas longer and so produce more generations of stars and have an higher metallicity. Davies & Phillipps (1989) showed that this can also be explained

[5] SNe-driven winds produced by an event of this kind would not blow away the gas of the galaxy, as shown in Section 7.2.

as a surface brightness–metallicity relation, in which there is a gas column density cut-off for star formation.

8 CONCLUSIONS

We have presented ($B - I$) colour and sensitive 21-cm observations of a sample of Virgo Cluster dwarf LSB galaxies that includes previously uncatalogued cluster members. These follow ups complete our work in paper I on the contribution of these galaxies to the faint-end slope of the LF. The H I observations also complete an earlier paper (Davies et al. 2004) aimed at investigating possible underevolved H I clouds in the cluster.

We find that, on average, colour trends are weak functions of both total B magnitude and central surface brightness of the galaxies. We have also compared the properties of dwarf galaxies in the cluster with those in other environments: dwarfs follow a similar density–morphology relation as for brighter galaxies. This is strange, given their predicted very different histories according to CDM theories (building blocks as opposed to fully assembled objects).

Cluster dwarfs are generally gas poor and red compared to dwarfs in the field, but they have average ($B - I$) colour and a velocity dispersion more like the spiral galaxy population.

The dwarfs in our sample do not seem to come from the infall of units like the Local Group: the dwarf-to-giant ratio is too high.

The cluster LF is steep while the H I mass function is shallow compared to the field.

Different mechanisms at work in the cluster environments were discussed and their relative efficiencies compared. We conclude that enhanced star formation activity owing to tidal interactions might account for the different properties of dwarfs in the different environments we compared. We believe that the dwarfs in our sample are not larger galaxies stripped of their gas or tidally transformed and have not been created in tidal interactions of larger galaxies.

The picture that we suggest is a scenario where tidal interactions play a fundamental role in triggering the star formation in cluster galaxies. We conclude that the dwarfs in our sample arrived (are arriving) in the cluster as gas-rich dwarfs converting their gas into stars rapidly. It is not clear to us how this might be accommodated within the CDM model.

ACKNOWLEDGMENTS

We want to thank the staff of Arecibo Observatory, especially Tapasi Ghosh, Phil Perillat and Chris Salter, for their help with the observations and data reduction. The Arecibo Observatory is part of the National Astronomy and Ionosphere Centre, which is operated by Cornell University under a cooperative agreement with the National Science Foundation. This research has made use of the GOLD Mine data base, operated by the Universita' degli Studi di Milano-Bicocca (Gavazzi et al. 2003), the Lyon-Meudon Extragalactic Data base, recently incorporated in HyperLeda, and the NASA/IPAC Extragalactic Data base, which is operated by the Jet Propulsion Laboratory, California Institute of Technology, under contract with the National Aeronautics and Space Administration.

REFERENCES

Abadi M. G., Moore B., Bower R. G., 1999, MNRAS, 308, 947
Adami C., Ulmer M. P., Durret F., Nichol R. C., Mazure A., Holden B. P., Romer A. K., Savine C., 2000, A&A, 353, 930
Andreon S., 1998, ApJ, 471, 694
Arnaboldi M., Aguerri J. A. L., Napolitano N. R., Gerhard O., Freeman K. C., Feldmeier J., Capaccioli M., Kudritzki R. P., 2002, AJ, 123, 760
Babul A., Rees M. J., 1992, MNRAS, 255, 346
Barnes J. E., Hernquist L., 1996, ApJ, 471, 115
Barton E. J., Geller M. J., Kenyon S. J., 2000, ApJ, 530, 660
Barton E. J., Geller M. J., Kenyon S. J., 2003, ApJ, 582, 668
Binggeli B., Sandage A., Tarenghi M., 1984, AJ, 89, 64
Binggeli B., Tammann G. A., Sandage A., 1987, AJ, 94, 251
Binggeli B., Popescu C. C., Tammann G. A., 1993, A&AS, 98, 275
Blitz L., Robishaw T., 2000, ApJ, 541, 675
Bothun G., Dressler A., 1986, ApJ, 301, 57
Butcher H., Oemler A., Jr, 1978, ApJ, 226, 559
Caldwell N., Rose J. A., Sharpless R. M., Ellis R. S., Bower R. G., 1993, AJ, 106, 473
Carey P. M., Gallagher J. S., Levine S. E., Aguilar L. A., 1996, A&AS, 188, 0607
Cavaliere A., Fusco-Femiano R., 1976, A&A, 49, 137
Chamaraux P., Balkowski C., Gerard E., 1980, A&A, 83, 38
Conselice J. C., 2002, ApJ, 573, 5
Conselice J. C., Gallagher J. S., Wyse R. F. G., 2001, ApJ, 559, 167
Conselice J. C., O'Neil K., Gallagher J. S., Wyse R. F. G., 2003a, ApJ, 591, 167
Conselice J. C., Gallagher J. S., Wyse R. F. G., 2003b, ApJ, 125, 66
Davies J., Phillipps S., 1989, Ap&SS, 157, 291
Davies J. et al., 2004, MNRAS, 349, 922
Dekel A., Silk J., 1986, ApJ, 303, 39
Dressler A., 1984, ARA&A, 22, 185
Dressler A., Gunn J. E., 1990, in Kron R., ed., ASP Conf. Ser. Vol. 10, Evolution of the Universe of Galaxies. Astron. Soc. Pac., San Francisco, p. 200
Dressler A., Thompson I. B., Shectman S. A., 1985, ApJ, 288, 481
Dressler A. et al., 1997, ApJ, 490, 577
Dressler A., Smail I., Poggianti B. M., Butcher H., Couch W. J., Ellis R. S., Oemler A., 1999, ApJS, 122, 51
Drinkwater M. J., Gregg M. D., Hilker M., Bekki K., Couch W. J., Ferguson H. C., Jones J. B., Phillipps S., 2003, Nat, 423, 519
Driver S. P., Couch W. J., Phillipps S., Smith R., 1998, MNRAS, 301, 357
Ferguson H. C., 1992, MNRAS, 255, 389
Ferguson H. C., Binggeli B., 1994, Astron. Astrophys. Rev., 6, 67
Ferguson H. C., Sandage A., 1991, AJ, 101, 765
Fioc M., Rocca-Volmerange B., 1997, A&A, 326, 950
Fukugita M., Shimasaku K., Ichikawa T., 1995, PASP, 107, 945
Gallagher J. S., Hunter D. A., 1984, ARA&A, 22, 37
Gallagher J. S., Wyse R. F. G., 1994, PASP, 106, 1225
Gavazzi G., Jaffe W., 1985, ApJ, 294, L89
Gavazzi G., Boselli A., Donati A., Franzetti P., Scodeggio M., 2003, A&A, 400, 451
Ghosh T., Salter C., 2002, in Stanimirovic S., Altschuler D., Goldsmith P., Salter C., eds, ASP Conf. Proc. Vol. 278, Single-Dish Radio Astronomy: Techniques and Applications. Astron. Soc. Pac., San Francisco, p. 521
Gnedin O. Y., 2003, ApJ, 582, 121
Graham J. A. et al., 1999, ApJ, 516, 626
Gregg M. D., West M. J., 1998, Nat, 396, 549
Gunn J. E., Gott J. R., 1972, ApJ, 176, 1
Hashimoto Y., Oemler J., Lin H., Tucker D. L., 1998, ApJ, 499, 589
Henriksen M. J., Byrd G., 1996, ApJ, 459, 82
Hoffman G. L., Helou G., Salpeter E. E., Sandage A., 1985, ApJ, 289, L15
Hoffman G. L., Helou G., Salpeter E. E., Lewis B. M., 1989, ApJ, 339, 812
Huchtmeier W. K., Karachentsev I. D., Karachentseva V. E., Ehle M., 2000, A&AS, 141, 469
Ichikawa S., Okamura S., Kodaira K., Wakamatsu K., 1988, AJ, 96, 62
Impey C., Bothun G., Malin D., 1988, ApJ, 330, 634
Jerjen H., Binggeli B., Barazza F. D., 2004, AJ, 127, 771
Kambas A., Davies J. I., Smith R. M., Bianchi S., Haynes J. A., 2000, MNRAS, 120, 1316
Karick A. M., Drinkwater M. J., Gregg M. D., 2003, MNRAS, 344, 188
Kauffmann G., White S., Guiderdoni B., 1993, MNRAS, 264, 201
Kennicutt R. C., 1983, ApJ, 272, 54

Kleyna J., Wilkinson M. I., Evans N. W., Gilmore G., Frayn C., 2002, MNRAS, 330, 792
Kodama T., Smail I., 2001, MNRAS, 326, 637
Larson R. B., 1986, MNRAS, 218, 409
Larson R. B., Tinsley B. M., 1978, ApJ, 219, 46
Lavery R. J., Henry J. P., 1988, ApJ, 330, 596
Lee H., McCall M. L., Richer M. G., 2003, AJ, 125, 2975
Leitherer C., Heckman T. M., 1995, ApJ, 96, 9
Liu C. T., Kennicutt R. C., 1995, ApJ, 450, 547
Lubin L. M., Postman M., Oke J. B., Ratnatunga K. U., Gunn J. E., Hoessel J. G., Schneider D. P., 1998, AJ, 116, 584
Mac Low M. M., Ferrara A., 1999, ApJ, 513, 142
Makarova L., 1999, A&AS, 139, 491
Marcolini A., Brighenit F., Ercole A., 2003, MNRAS, 345, 1329
Mateo M., 1998, ARA&A, 36, 435
Matthews L. D., Gallagher J. S., III, 1997, AJ, 114, 1899
Mayer L., Moore B., 2004, MNRAS, 354, 477
Merritt D., 1984, ApJ, 276, 26
Mihos J. C., Hernquist L., 1996, ApJ, 464, 641
Milne M. L., Pritchet C. J., 2002, A&AS, 201, 4211
Miralda-Escude J., 2003, Sci, 300, 1904
Moore B., 2003, in Mulchaey J. S., Dressler A., Oelmer A., eds, Canergie Observatories Astrophysics Series, Vol. 3, Cluster of Galaxies: Probes of Cosmological Structure and Galaxy Evolution. Cambridge Univ. Press, Cambridge
Moore B., Lake N., Katz N., 1998, ApJ, 495, 139
Moore B., Lake G., Quinn T., Stadel J., 1999, MNRAS, 304, 465
Noguchi M., Ishibashi S., 1986, MNRAS, 219, 305
Norberg P. et al., 2002, MNRAS, 336, 907
Oh K. S., Lin D. N. C., 2000, ApJ, 543, 620
Okazaki T., Taniguchi Y., 2000, ApJ, 543, 149
O'Neil K., Bothun G. D., Schombert J., 1998, AJ, 116, 2776
Persic M., Salucci P., Stel F., 1996, MNRAS, 281, 27
Poggianti B. M., Smail I., Dressler A., Couch W. J., Barger A. J., Butcher H., Ellis R. S., Oemler A., 1999, ApJ, 518, 576
Poggianti B. M., Bridges T. J., Mobasher B., Carter D., Doi M., Iye M., Kashikawa N., Komiyama Y., 2001, ApJ, 562, 269
Pritchet C. J., van der Bergh S., 1999, AJ, 118, 883
Rakos K., Schombert J., 2004, AJ, 127, 1502
Reed B., 1985, PASP, 97, 120
Roberts M. S., 1968, AJ, 73, 945
Roberts S., Davies J., Sabatini S., Baes M., Linder S., Smith R., Evans R., 2004, MNRAS, 352, 478
Sabatini S., Davies J., Scaramella R., Smith R., Baes M., Linder S. M., Roberts S., Testa V., 2003, MNRAS, 341, 981 (paper I)
Schindler S., Binggeli B., Böhringer H., 1999, A&A, 343, 420
Schombert J. M., Pildis R. A., Eder J. A., 1997, ApJS, 111, 233
Schulz S., Struck C., 2001, MNRAS, 328, 185
Secker J., Harris W. E., 1996, ApJ, 469, 623
Secker J., Harris W. E., Cote P., Oke J. B., 1998, A New Vision of an Old Cluster: Untangling Coma Berenices. World Scientific, Singapore
Solanes J. M., Manrique A., Garcia-Gomez C., Gonzalez-Casado G., Giovannelli R., Haynes M. P., 2001, ApJ, 548, 97
Solanes J. M., Sanchis T., Salvador-Solé E., Giovanelli R., Haynes M. P., 2002, AJ, 124, 2440
Spergel D. N., Verde L., Peiris H. V., Komatsu E., Nolta M. R., Bennett C. L., Halpern M., Hinshaw G., 2003, ApJS, 148, 161
Trentham N., Hodgkin S., 2002, MNRAS, 333, 423
Trentham N., Tully R. B., 2002, MNRAS, 335, 3
Trentham N., Tully B., Verheijen M. A. W., 2001, MNRAS, 325, 385
Tully B. R., Verheijen M. A. W., Pierce M. J., Huang J. S., Wainscoat R. J., 1996, AJ, 112, 2471
Tully B. R., Somerville R. S., Trentham N., Verheijen M. A. W., 2002, ApJ, 569, 573
Valluri M., Jog C. J., 1991, ApJ, 374, 103
van Gorkom J. H., 2003, in Mulchaey J. S., Dressler A., Oemler A., eds, Clusters of Galaxies: Probes of Cosmological Structure and Galaxy Evolution. Cambridge Univ. Press, Cambridge
van Zee L., 2001, AJ, 121, 2003
Vilchez-Gomez R., Bruzual G., Pello R., Dominguez R., 2001, Ap&SS, 276, 757
Vollmer B., Cayatte V., Balkowski C., Duschl W. J., 2001, ApJ, 561, 708
Young J. F., Kenney J. D., Tacconi L., Claussen M. J., Huang Y. L., Tacconi-Garman L., Xie S., Schloerb F. P., 1986, ApJ, 311, 17
White S., Frenk C., 1991, ApJ, 379, 52
White S., Rees M., 1978, MNRAS, 183, 341
Worthey G., 1994, ApJS, 95, 107

This paper has been typeset from a TEX/LATEX file prepared by the author.